NOVEL MULTI-STEP REGION GROWING ALGORITHM FOR THE SEGMENTATION OF BURN IMAGES

C. Serrano*, B. Acha* and I. Fondón*

* Dept. de Teoría de la Señal y Comunicaciones, University of Seville, Seville, Spain

cserrano@us.es, bacha@us.es, heiwa78@hotmail.com

Abstract: In this paper, a novel region growing algorithm for segmenting burn wounds in digital photographs of the skin is presented. This segmentation step has been developed as part of a CAD tool for burn diagnosis. During the region growing the inclusion condition relies on a tolerance parameter, which is adaptively determined. It initially has a low value and this is recursively increased until a stop condition is reached. This condition is based on the analysis of the statistical distribution of the pixels within the grown region. The great advantage of the method is that it does not rely on fine-tune parameters. The algorithm has been tested with 44 images of burn wounds obtaining very good results. Its performance has been measured quantitatively by comparing it with a ground truth obtained from the manual segmentation of five experts.

Introduction

For a successful evolution of a burn injury it is essential to initiate the correct first treatment [1]. To choose an adequate one, it is necessary to know the depth of the burn, and a correct visual assessment of the burn depth highly relies on specialized dermatological expertise. As the cost of maintaining a Burn Unit is very high, it would be desirable to have an automatic system to give a first assessment in all the local medical centres, where there is a lack of specialists [2]. The World Health Organization demands that, at least, there must be one bed in a Burn Unit for each 500000 inhabitants. So, normally, one Burn Unit covers a large geographic extension. If a burn patient appears in a medical centre without Burn Unit, a telephone communication is established between the local medical centre and the closest hospital with Burn Unit, where the not-expert doctor describes subjectively the colour, shape and other aspects considered important for burn characterization. The result in many cases is the application of an incorrect first treatment (very important, on the other hand, for a correct evolution of the wound), or unnecessary displacements of the patient, involving high sanitary cost and psychological trauma for the patient and family. Therefore, it would be desirable that a CAD tool for automatic diagnosis were available in those medical centres without specialists.

In a previous work [3] a CAD tool for assessing the depth of burns was developed. For this purpose, two main steps were performed: the segmentation of the burned wound and the classification of its depth.

Automatic image segmentation is one of the fundamental problems of early computer vision. If any error occurs during this step, the whole process will fail irremediably, that is, an effective segmentation can usually dictate eventual success of the analysis. This is the reason why segmentation is a matter that has been studied by many researchers all over the world [4]. In this paper, in order to improve the success rate in the classification obtained in [3], a new segmentation algorithm is proposed.

Conventional segmentation techniques for images can be classified into four categories. One is region-based, which relies on the homogeneity of spatially localized features [5, 6]. The second one is boundary based and it consists of finding a boundary using discontinuity measures [7, 8]. The third one is the thresholding technique, which is based on the assumption that pixels whose value lies within a certain range belong to the same class [9, 10]. Finally, hybrid techniques integrate the results of boundary detection and region growing expecting to provide in this way a more accurate segmentation of images. Region growing is a region-based technique which has been widely accepted [11] because of its capacity to combine both global and spatial information.

In this paper we propose a novel region-growing technique for image segmentation, which has the main advantage of not having any tuning parameter. It is based on progressively increasing the tolerance parameter of the region growing until a certain condition is met. The condition is that the distribution of the region obtained with this tolerance is the most similar to a Rayleigh one, according to the Bhattacharyya distance.

To adapt the algorithm to segment color images, a conversion from a three-color-plane image to a one-plane image is performed. In this conversion Euclidean distance to a color target in the $L^*u^*v^*$ color space is performed. This conversion is based on the fact that Euclidean distances in the $L^*u^*v^*$ color space are consistent with perceived color differences [12].

Method

ISSN: 1727-1983

Preprocessing and conversion to one-plane image: As it is well known, segmentation algorithms strongly depend on the application. In this sense, the detail level of the segmentation has to be chosen according to the final use this segmentation result will have. The application that the algorithm will have requires that physicians may take part in the process. In this sense, the user will select a small selection box in the region to be segmented as a first step, in order to indicate the type of burn to be classified (it should be noted that in the same photograph could appear different types of burns).

For homogenizing purposes, an anisotropic diffusion filter [13, 14] is applied to the image and the selection box. The choice of this filter is due to its property of preserving the boundaries within the image.

After this step, a gray-scale image is obtained from the diffused color image. In this gray-scale image, differences between the burnt skin selected by the user and other parts of the image are emphasized. Based on the observation that physicians segment burn wounds by measuring differences among colors, for each pixel in the image the following operation is performed [15]:

$$f(n,m)=\sqrt{\left(L^*(n,m)-L^*_{ref}\right)+\left(u^*(n,m)-u^*_{ref}\right)+\left(v^*(n,m)-v^*_{ref}\right)} \qquad (1)$$

where $L^*(n,m),u^*(n,m),v^*(n,m)$ are the coordinates of a pixel in the position (n,m) in the $L^*u^*v^*$ diffused color image and $L^*_{ref}, u^*_{ref}, v^*_{ref}$ is the centroid of the area selected by the user (selection box) in the $L^*u^*v^*$ color space.

Finally, due to the fact that colors of healthy skin and burns are very similar between them, a contrast enhancement is applied to the histogram of the distance image.

Multistep region growing algorithm: The multi-step region-growing algorithm starts by choosing the seeds. It should be outlined that, in the gray-scale image, the region to be segmented should have the lowest pixel values, as it represents a distance image. Seeds must belong to the region of interest, so they will have low values. In order to select them, the following steps are followed: 1) Selection of the local minima of the image, which represent the candidates to seeds. Not all these candidates will be seeds of the region-growing because these local minima do not belong necessarily to the region of interest. 2) Application of a threshold to these candidate seeds. The threshold is determined from the histogram of the distance image, more specifically, the threshold will be the position of the peak closest to the left part of the histogram, as seeds should have low values as explained before. The procedure to find significant peaks and valleys follows the thresholding algorithm explained in [3]. In Figure 1 an example about how seeds are selected is shown. Firstly, the minima in the distance image are selected. They constitute the candidates to seeds. After the thresholding, the definitive seeds are found.

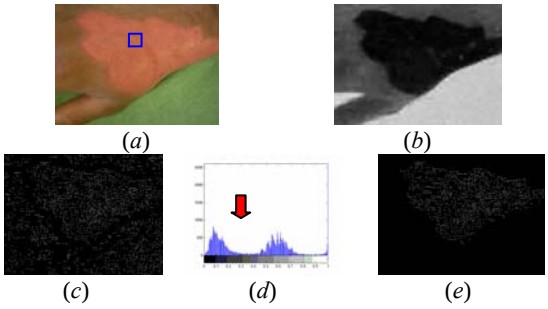

Figure 1: Seed selection process. (*a*) Original image with the selection box indicated by the user shown in blue. (*b*) Distance image. Image (*c*) shows the local minima of the color distance image. In (*d*) the thresholding of the histogram is illustrated, where the threshold is shown with a red arrow. And the seeds are obtained in (*e*).

Once the seeds are selected, the 4-neighbor pixels of each seed are examined to be included in the region. The two inclusion conditions are: 1) the pixel has not been previously included in the region and 2) the value of the pixel is within certain tolerance range, that is, $0 \le f(i,j) \le \tau$, where $f(i,j)$ is the distance image, (i,j) represents the coordinates of any of the 4-neighbor pixels, and τ (>0) is the step of tolerance parameter, gradually increased until it reaches its optimum value. It should be noted that it is a distance image, where pixels belonging to the burn are those closer to zero.

To determine the stop condition, we have observed that within an object the distribution of the pixel values follows approximately a Rayleigh one, whereas when a region begins to include other parts of the image the distribution tends to grow differently from a Rayleigh. Likewise, when the region is included in an object but only embraces it partially, the distribution of the pixel values tends to have a distribution whose right tail has less weight than the one of a Rayleigh distribution. Nevertheless, as the borders of the region are getting closer to the actual border of the object, the tail of the distribution grows, so the distribution tends to a Rayleigh one. The reason is that the change of the color in the borders of an object is progressive. Therefore, the tolerance can be chosen as the one which provides a region whose distribution best matches a Rayleigh one. In Figure 2 one example is presented, which corroborates this observation. In Figures *b, e* and *h* the histograms of the regions marked in pink color in Figures *a*, *d* and *g* are presented. In Figures *c*, *f* and *i* the histograms of a Rayleigh distribution adapted to the mean and variance of the histograms in *b, e* and *h* respectively are shown. As can be observed in those figures, the histogram of a region within an object but smaller than this one tends to be sharper than a Rayleigh. When the region includes more pixels than those belonging to the object, a second peak tends to appear in the histogram and, therefore, the distribution tends to grow differently from a Rayleigh one. On the other hand, as can be seen in Figures *b* and *c*, the

ISSN: 1727-1983

histogram of Figure *b* fits pretty well the Rayleigh distribution shown in Figure *c*.

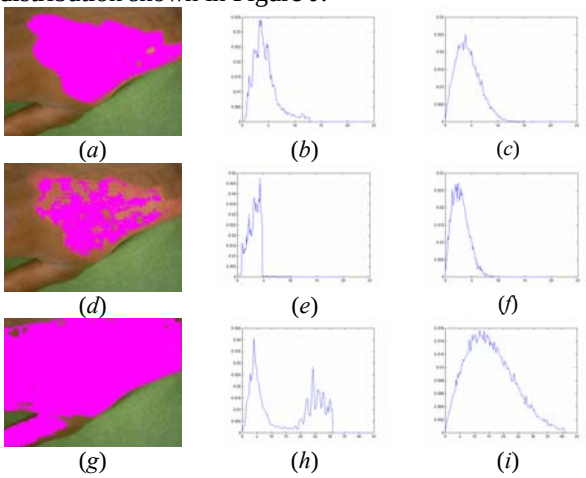

Figure 2: In Figures *b*, *e* and *h* the histograms of the regions selected in pink color from Figures *a*, *d* and *g* are shown. In Figures *c*, *f* and *i* the histograms of a Rayleigh distribution with the mean and variance adapted to the ones of Figures *b*, *e* and *h* are shown.

In order to find the optimum step of tolerance, we use the Bhattacharyya distance [16] as a tool to compare two distributions. The Bhattacharyya distance measures the distance between two statistical distributions.

First of all, the histogram of the region grown with the actual tolerance is calculated (h_S). Secondly, the Rayleigh parameter is estimated from the pixels belonging to the region as:

$$b = \sqrt{\frac{1}{2L}\sum_{(n,m)\in region} f^2(n,m)} \qquad (2)$$

where L is the number of pixels in the region and $f(n, m)$ is the pixel value of the distance image in the position (n, m). The Rayleigh parameter defines the Rayleigh distribution as indicated in the following equation:

$$p(x) = \frac{x}{b^2}\exp\left(\frac{-x^2}{2b^2}\right) \qquad (3)$$

where $p(x)$ is the Rayleigh probability density function. From this Rayleigh parameter, a histogram is generated (h_R).

Finally, the Bhattacharyya distance between the two histograms is calculated as:

$$d = -\ln\left(\sum_i \sqrt{h_R(i)\cdot h_S(i)}\right), \qquad (4)$$

where i indexes the bins of the normalized histograms of the Rayleigh distribution, h_R, and of the region, h_S. The optimum value of the tolerance will be chosen as the one which minimizes the Bhattacharyya distance.

Results

The algorithm has been tested with 44 burn images obtaining an accurate segmentation in all the cases. The database was formed following a protocol [2] and the images were calibrated. Figure 3 shows some segmentation results. It should be noted the difficulty in segmenting them due to the similarity between colors of burn wounds and healthy skin. Figure 3a presents a superficial dermal burn, and Figure 3c shows a full-thickness one. In both images the selection box indicated by the user is shown in blue.

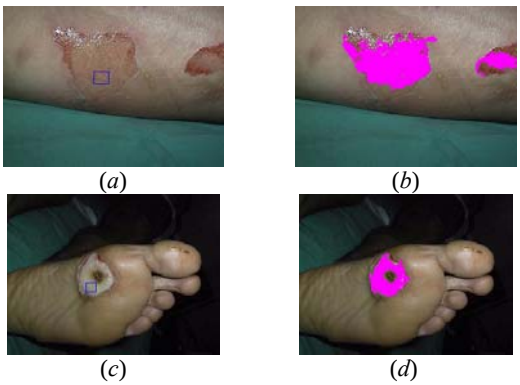

Figure 3: Examples of the segmentation (selection box is indicated in blue). (*a*) Superficial dermal burn. (*b*) Segmentation of (*a*). (*c*) Full thickness burn. (*d*) Segmentation of (*c*).

In order to measure the performance of the segmentation algorithm, all the images from the database were segmented by 5 medical experts[1]. We computed a probabilistic estimate of the ground truth (gold standard) applying an Expectation-Maximization algorithm [17] based on a group of expert segmentations. Two parameters were obtained for each image in the comparison. The first one was the *Positive Predictive Value* (*PPV*), which measures the ratio between the number of pixels segmented by the algorithm which fit the segmentation gold standard and the total amount of pixels segmented by the algorithm. The second parameter is called *Sensitivity* (*S*), and it is the ratio between the number of pixels segmented by the algorithm which fit the segmentation gold standard and the total amount of pixels in the segmentation gold standard. Intuitively it can be seen that the first parameter measures the over-segmentation, which would be null if *PPV* were 1. Likewise, *S* measures the under-segmentation. These two parameters are summarized in equation:

$$PPV = \frac{TP}{TP+FP}, \qquad Sensitivity = \frac{TP}{TP+FN}, \qquad (5)$$

where *TP* means True Positives, that is, pixels which, belonging to the region segmented by experts, were

[1] All of them are plastic surgeons affiliated to the Burn Unit of the Hospital Universitario Virgen del Rocío (Seville, Spain).

ISSN: 1727-1983

segmented by the algorithm; *FN* means False Negatives, that is, pixels which, belonging to the segmented region, were not segmented by the algorithm; and *FP* means False Positives, that is, pixels which, not belonging to the segmented region, were segmented by the algorithm.

In Table 1 a summary of the results is shown. It presents the mean of the Sensitivity and PPV parameters for the 44 images of the database. As can be seen, the results are very good, especially if we take into account that colors of burn wounds are, very often, very similar to healthy skin.

Table 1: Summary of *S* and *PPV* parameters for 44 images of burn wounds.

	Sensitivity (*S*)	***PPV***
Multi-step algorithm	0.8200	0.8607

Conclusions

In this paper a new segmentation algorithm based in a multi-step region growing technique is presented. This algorithm is applied to burn color images. The good results attained have been quantified by calculating two parameters which take into account the segmentation performed by 5 experts in the field.

The segmentation algorithm is developed as part of a CAD tool for classifying burns into their depth. We have focused our attention in improving the segmentation algorithm as it represents a crucial step in the CAD burn tool. This improvement in the segmentation algorithm will allow attaining better classification results because the input parameters to the classifier are obtained from the segmented region.

Acknowledgements

The authors thank the Burn Unit of Virgen del Rocío Hospital, Seville (Spain), their invaluable help, for providing us the burn wound photographs and their medical advice, and the CICYT (Spain) for financial support (project TIC-2002-01401).

References

[1] CLARKE, J.A. (1992): 'A Colour Atlas of Burn Injuries', (Chapman & Hall Medical, London)

[2] ROA, L.M., GÓMEZ-CÍA T., ACHA B., and SERRANO C. (1999): 'Digital Imaging in Remote Diagnosis of Burns', *Burns*, **7,** pp. 617-624

[3] ACHA B., SERRANO C., ACHA J.I., and ROA L.M. (2003): 'CAD Tool for Burn Diagnosis', *Lectures Notes in Computer Science: Information Processing in Medical Imaging*, **2732**, pp. 294-305.

[4] HARALICK R.M., and SHAPIRO L. G. (1985): 'Image segmentation techniques', *Comput. Vision Graphics Image Processing*, **29,** pp. 100-132

[5] FAN J., YAU D. K. Y., ELMAGARMID A.K., and AREF W. G. (2001): 'Automatic image segmentation by integrating color-edge extraction and seeded region growing' *IEEE Trans. Image Processing*, **10**, n. 10, pp. 1454-1466

[6] REYNOLDS R. G., and ROLNICK S. R. (1995)**: '**Learning the parameters for a gradient-based approach to image segmentation from the results of a region growing approach using cultural algorithms', IEEE International Conference on Evolutionary Computation, **2**, p. 819 -824.

[7] BHANDARKAR S. M., and SIEBERT A. (1992): 'Integrating edge and surface information for range image segmentation', Proc. IEEE Southeastcon, **1**, p. 106 -113.

[8] SABER E., TEKALP A. M., and BOZDAGI G. (1996): 'Fusion of color and edge information for improved segmentation and edge linking', Proc. IEEE Int. Conf. on Acoustics, Speech, and Signal Processing, **4**, p. 2176 -2179

[9] TOBIAS O.J., and SEARA R. (2002): 'Image segmentation by histogram thresholding using fuzzy sets', *IEEE Transactions on Image Processing*, **11** n. 12, pp. 1457 -1465

[10] SEKITA I., KURITA T., OTSU N., and ABDELMALEK N. (1994): 'A thresholding method using the mixture of normal density functions', Proc. Int. Symp. Speech, Image Processing and Neural Networks, **1**, p. 304-307

[11] WAN S. Y., and HIGGINS W. E. (2003): 'Symmetric region growing', *IEEE Transactions on Image Processing*, **12** n. 9, pp. 1007 -1015

[12] WYSZECKI G., and STILES W.S. (1982): 'Color Science: Concepts and Methods, Quantitative Data and Formulae', (WILEY, New York)

[13] PERONA P., and MALIK J. (1990): 'Scale-Space and Edge Detection using Anisotropic Diffusion', *IEEE Trans. on Pattern Analysis and Machine Intelligence*, **12**, n. 7, pp. 629-639

[14] LUCCHESE L., and MITRA S.K. (2001): 'Color Segmentation Based on Separate Anisotropic Diffusion of Chromatic and Achromatic Channels' IEE Proceedings Vision, Image and Signal Processing, **148,**n. 3, p. 141-150

[15] ACHA B., SERRANO C., and ACHA J.I. (2002): 'Segmentation of Burn Images Using the $L^*u^*v^*$ Space and Classification of their Depths by Color and Texture Information', SPIE Int. Symposium on Medical Imaging, San Diego (CA, USA.), **4684,** Part Three p. 1508-1515

[16] FUKUNAGA K. (1990).: 'Introduction to Statistical Pattern Recognition'. 2nd edition, (MORGAN KAUFMANN ACADEMIC PRESS, San Diego, CA)

[17] WARFIELD S.K., ZOU K.H., and WELLS W.M. (2002): 'Validation of image segmentation and expert quality with an expectation-maximization algorithm'. MICCAI 2002 Fifth Int. Conf. on Medical Image Computing and Computer Assisted Intervention, Tokyo (Japan), p. 298-306

ISSN: 1727-1983